

Resonant thermal transport in semiconductor barrier structures

P. Hylgaard

Department of Applied Physics, Chalmers University of Technology, SE-41296 Göteborg, Sweden
 (Received 20 October 2003; revised manuscript received 21 January 2004; published 24 May 2004)

I report that thermal single-barrier (TSB) and thermal double-barrier (TDB) structures (formed, for example, by inserting one or two regions of a few Ge monolayers in Si) provide both a suppression of the phonon transport as well as a resonant-thermal-transport effect. I show that high-frequency phonons can experience a traditional double-barrier resonant tunneling in the TDB structures while the formation of Fabry-Perot resonances (at lower frequencies) causes quantum oscillations in the temperature variation of both the TSB and TDB thermal conductances σ_{TSB} and σ_{TDB} .

DOI: 10.1103/PhysRevB.69.193305

PACS number(s): 66.70.+f, 44.10.+i, 63.20.-e, 42.25.Hz

The understanding of phonon transport in nanoscale heterostructured materials¹ is in an exciting development motivated in part by the search to improve both thermoelectric² and thermoionic³ cooling. The interest also derives from the observation that nanostructure phonons exhibit nanoscale-transport, confinement, and quantization effects similar to those observed for electrons and photons. A significant suppression is observed^{4,5} in the in-plane thermal conductivity of heterostructures and is explained by interface scattering as a phonon Knudsen-flow effect.^{6,7} Similarly, the perpendicular thermal conductivity κ_{SL} of semiconductor superlattices shows a dramatic reduction^{8,9} (compared to the average bulk conductivities) that cannot be accounted for alone by the expected decrease¹⁰ in the effective superlattice-phonon lifetime τ_{SL} . Instead, the strong reduction in $\kappa_{\text{SL}}/\tau_{\text{SL}}$ results from a pronounced miniband formation where the difference in materials hardness forces an increasing confinement of modes with a finite in-plane momentum to either the Si or Ge layers in the superlattice.¹¹ Finally, the phonon quantum-point-contact effect in nanoscale dielectric wires¹² shows that the phonon wave nature also directly affects the low-temperature phonon transport.

Here I extend the search for quantized thermal-transport effects in semiconductor nanostructures to finite temperatures. I focus on the phonon conduction across Si/few-Ge-monolayers/Si thermal single-barrier (TSB) and corresponding Si/Ge/Si/Ge/Si thermal double-barrier (TDB) heterostructures. I document (i) a strong suppression of the phonon-transport thermal conductances σ_{TSB} and σ_{TDB} , (ii) a traditional type of double-barrier resonant tunneling for high-frequency phonons in the TDB structures, and (iii) that phonon Fabry-Perot resonances¹³ (at lower frequencies) produce a resonant-thermal-transport effect at finite temperatures in both the TSB and TDB structures (for sufficiently small Ge-barrier thicknesses). My focus is on the technology relevance rather than the low-temperature transport. Instead of the long-wavelength phonon analysis of Ref. 12, I therefore present a phonon-model calculation of the (resonant) thermal transport which remains applicable at finite frequencies, includes the phase-space limitations imposed by total-internal reflection, and describes the important effect of increasing misalignment of the Si-/Ge-phonon dynamics as the in-plane momentum q increases.¹¹ The prediction (iii) bridges the concept of thermal-transport quantization effects

from the previous focus on low-temperature phonon transmission¹² to the finite-temperature nanostructure heat conduction for which I show that oscillations persist up to temperatures $\Theta \approx 50$ K.

To emphasize the potential technological relevance I first report a simple estimate for the thermal-conductance suppression in two examples of TSB and TDB structures, Fig. 1, formed as a Si/triple-Ge-monolayer/Si and as a Si/2Ge/3Si/2Ge/Si semiconductor heterostructure, respectively. I predict below a strong high-temperature suppression

$$\sigma_{\text{TSB,TDB}} \sim \sigma_K \lesssim 10^4 \text{ W/Kcm}^2 \quad (1)$$

specified by the single-Si/Ge interface Kapitza conductance¹⁴ $\sigma_K(\Theta) \leq \sigma_K(\Theta \rightarrow \infty) \approx 10^4 \text{ W/Kcm}^2$ (as also obtained in my phonon-model calculation). The thermal-conductance estimate (1) results by describing the full dynamics of phonons that approach an individual single-barrier/double-barrier structure (rather than moving in a superlattice) and therefore provides a more consistent description than the so-called ef-

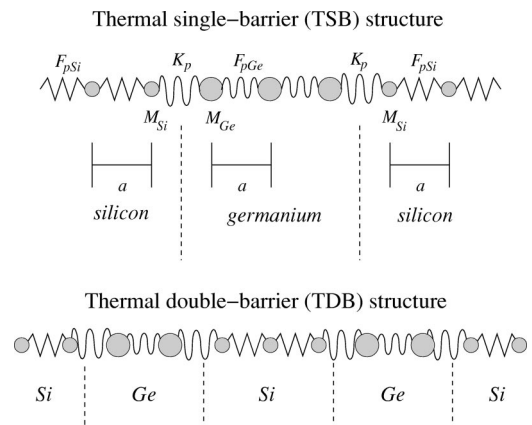


FIG. 1. Sample realization of thermal barrier structures in which even a few monolayers of a softer material (here germanium) serve to inhibit the otherwise effective (phonon) thermal transport in surrounding hard materials (here Si). The figure shows examples of both thermal single-barrier (TSB) and thermal double-barrier (TDB) heterostructures that exhibit a resonant-thermal transport effect. The figure also shows schematics of the phonon model used to calculate the finite-temperature variation of the TSB and TDB thermal conductances.

fective conductance⁹ $G_{\text{SL}} \equiv \kappa_{\text{SL}}(d)/(d/2) \sim 10^5$ W/Kcm² extracted⁹ from measurements (at $\Theta = 200$ K) of the thermal conductivity $\kappa_{\text{SL}}(d)$ in Si/Ge superlattices with a nanoscale periodicity d . The estimate (1) shows that repeating the TSB or TDB formation every 50 nm provides a reduction of the effective thermal conductivity κ to the value of a Si/Ge alloy $\kappa_{\text{alloy}} \approx 5$ W/Km (repetition every 5 nm would be needed if the limit $\sigma_{\text{TSB}} \leq G_{\text{SL}}$ applies).

The TSB and TDB structures also give rise to a resonant-thermal-transport effect which is observable at finite temperatures ($\Theta \leq 50$ K). Figure 1 shows a schematics of the phonon model which I here solve to calculate the phonon tunneling and the resulting thermal conductance across both a single interface and across the repeated interfaces in the TSB and TDB structures. I assume a shared silicon (germanium) lattice constant a , the atomic masses $M_{\text{Si(Ge)}}$, and intrasilicon (intragermanium) force constants $F_{p;\text{Si(Ge)}}$ and interlayer coupling constant $K_p \equiv (F_{p;\text{Si}}F_{p;\text{Ge}})^{1/2}$ specified by the materials sound velocities.¹¹ The tunneling¹⁵ of phonon modes that are polarized and propagating in the perpendicular \hat{z} -direction is well described within such a one-dimensional lattice model. I refer to our previous investigation of superlattice thermal transport¹¹ for a description of how I include the effects of a finite in-plane momentum within a simple-cubic model by adding in-plane force constants $F_{t;\text{Si(Ge)}}$ and corresponding characteristic frequencies $\Omega_{p,t;\text{Si(Ge)}} \equiv (4F_{p,t;\text{Si(Ge)}}/M_{\text{Si(Ge)}})^{1/2}$; Fig. 1 of Ref. 11. The set of force constants $F_{p,t;\text{Si(Ge)}}$ also specifies the phonon-transport contributions from $\xi_{\hat{x},\hat{y}}|\hat{x},\hat{y}$ -polarized heterostructure phonons¹⁶ and these modes are, of course, also included in the transport calculation. Below I limit the formal discussion to the contributions from $\xi_{\hat{z}}|\hat{z}$ -polarized modes which for a given in-plane momentum \vec{q} can be characterized by the dimensionless in-plane energy measure¹¹ $0 < \alpha_{\vec{q}} \equiv [2 - \cos(q_x a) - \cos(q_y a)] < 4$. This measure is, like the frequency, conserved¹¹ across the heterostructure interfaces in this phonon-transport model study.

Figure 2 reports my calculations of the phonon transmission in the single-interface, TSB, and TDB structures. Starting from the model equations of motion for every atom and adapting the approach of Ref. 14, I determine the single-interface, TSB, and TDB transmission probabilities $T_{\text{K,TSB,TDB}}(\omega, \alpha_{\vec{q}})$ as a function of the phonon frequency and (conserved) in-plane momentum q . The figure reports a comparison of $T_{\text{K}}(\omega, \alpha_{\vec{q}=0})$ and $T_{\text{TDB}}(\omega, \alpha_{\vec{q}=0})$ and identifies the onset (vertical dashed-dotted line) when incoming Si phonons become attenuated in the Ge barriers. The figure documents that the TDB structure supports a traditional type of phonon (double-barrier) resonant tunneling at high frequencies ($\omega_{>}$) when the phonon dynamics in Ge is attenuated [and $T_{\text{K}}(\omega_{>}) = 0$]. The figure also illustrates that both the TDB and TSB structures support a number of Fabry-Perot resonances at lower frequencies ($\omega_{<}$) when the individual interfaces provide partial transmission [i.e., when $0 < T_{\text{K}}(\omega_{<}) < 1$].

To clarify the nature and measurability of the high-frequency resonant tunneling, I summarize the model calculations of the phonon dynamics at general in-plane momen-

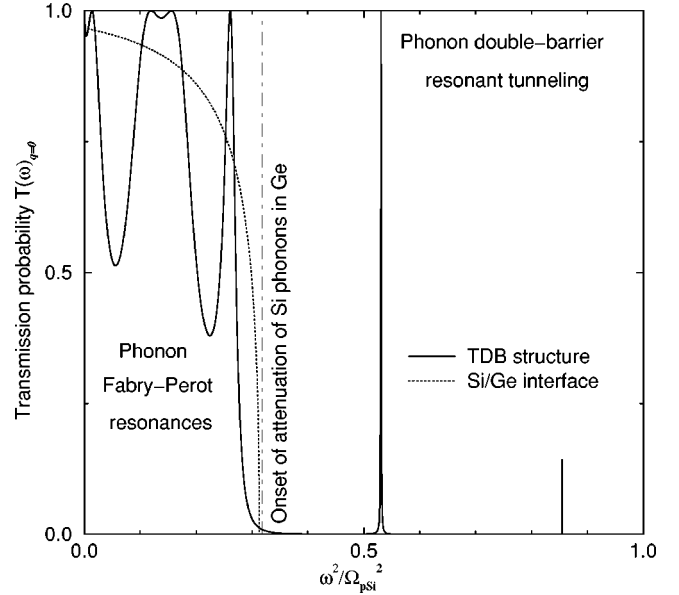


FIG. 2. Comparison of calculated phonon transmission probability (evaluated at in-plane momentum $q=0$) for the Si/Ge thermal double-barrier structure, Fig. 1 (solid curve) and for the individual Si/Ge interface (dotted curve). The vertical line identifies the frequency-squared value above which incoming Si phonons become attenuated in Ge. The TDB structure is seen to support a traditional type of double-barrier resonant tunneling above this limit (when the Ge-layers represent actual barriers) but also multiple Fabry-Perot resonances (at lower frequencies) when incoming phonons experience a partial transmission at each of the individual Si/Ge interfaces. Note that the TDB's (and TSB's) naturally become completely transparent as $\omega \rightarrow 0$.

tum, $\alpha_{\vec{q}} \neq 0$. I note that bulk silicon (germanium) phonon propagation at a given $\alpha_{\vec{q}}$ requires that the frequency square exceeds $\omega_{\text{Si(Ge),min}}^2(\alpha_{\vec{q}}) \equiv \Omega_{t;\text{Si(Ge)}}^2(\alpha_{\vec{q}}/2)$ but remains bounded by $\omega_{\text{Si(Ge),max}}^2(\alpha_{\vec{q}}) \equiv \Omega_{t;\text{Si(Ge)}}^2(\alpha_{\vec{q}}/2) + \Omega_{p;\text{Si(Ge)}}^2$.¹¹ The finite silicon/germanium acoustic mismatch ensures that $\omega_{\text{Si,min}[\text{max}]}(\alpha_{\vec{q}}) > \omega_{\text{Ge,min}[\text{max}]}(\alpha_{\vec{q}})$. Phonon propagation (i.e., absence of attenuation) in *both* silicon and germanium layers thus effectively requires that

$$\omega_{\text{Si,min}}^2(\alpha_{\vec{q}}) < \omega^2 < \omega_{\text{Ge,max}}^2(\alpha_{\vec{q}}), \quad (2)$$

since this is the condition for an incoming silicon phonon to avoid total internal reflection at an individual Si/Ge interface (as formulated in the present model study). The condition (2) is a severe phase-space restriction which, for example, becomes *impossible* to satisfy at $\alpha_{\vec{q}} > 2$ in Si/Ge structures.¹¹ For incoming Si phonons with a frequency ω above the onset of Ge attenuation, the model study yields a strong exponential decay $1/\gamma_{\text{Ge}} \sim a$, a vanishing single-barrier transmission ($T_{\text{TSB}} \rightarrow 0$), and the strongly peaked double-barrier resonant-tunneling transmission T_{TDB} that is illustrated in Fig. 2. The high-frequency resonant tunneling may become observable¹⁵ if it is possible to design a frequency-selective source of terahertz phonons.¹⁷ However, for a thermal distribution $N(\omega, \Theta)$ of incoming Si phonons at a relevant elevated temperature Θ , I find the phase-space contribution from the

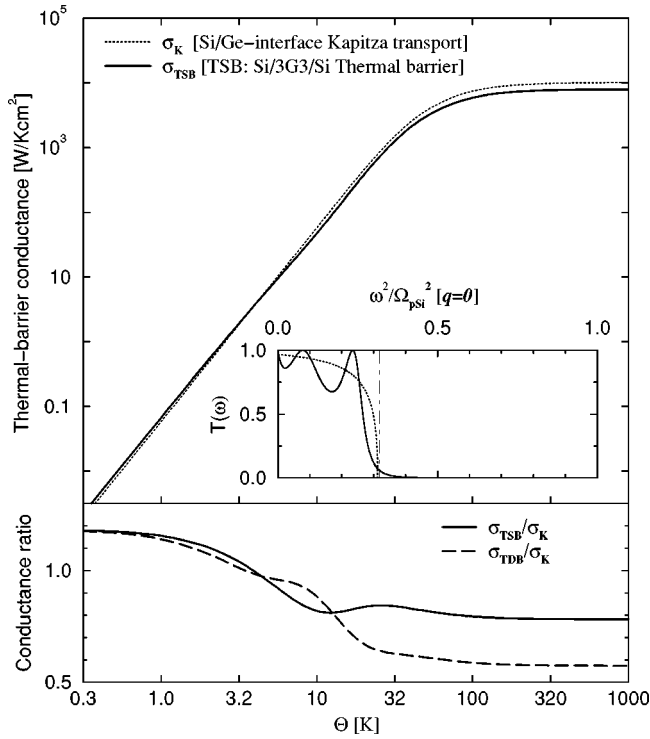


FIG. 3. Temperature dependence of (perpendicular) thermal conductance σ_{TSB} (solid curve) for a Si/3Ge/Si TSB heterostructure compared with the Si/Ge-interface Kapitza conductance $\sigma_K \equiv \sigma_{\text{Si/Ge}}$ (dotted curve). The thermal barrier transport is effectively subject to similar severe phase-space restrictions (enforced by total internal reflection) as the single-interface conductance and can thus be estimated $\sigma_{\text{TSB}}(T) \sim \sigma_K(T)$. The insert panel compares the TSB phonon transmission probability $T_{\text{TSB}}(\omega) \equiv T_{\text{TSB}}(\omega; \alpha_q = 0)$ (solid curve) and the single-Si/Ge transmission probability (dotted curve) at zero in-plane momentum, $q = 0$. The barrier transmission is seen to be essentially eliminated above the frequency (vertical dashed-dotted line) when the incoming phonon must tunnel across the Ge barrier layers. At the same time, the barrier transmission T_{TSB} also shows clearly defined low-energy phonon Fabry-Perot resonances (similar to those of the T_{TDB} , Fig. 2) produced within the 3Ge barrier. The bottom panel documents how the set of lower-energy Fabry-Perot resonances produce quantum oscillations in the TSB and TDB conductance ratios $\sigma_{\text{TSB}}/\sigma_K$ (solid curve) and $\sigma_{\text{TDB}}/\sigma_K$ (dashed curve).

(high-frequency) resonant tunneling, Fig. 2, too small to directly affect the TDB thermal conductance.

In contrast, I find that the phonon Fabry-Perot resonances do produce observable finite-temperature quantization effects in the TDB and TSB heat conduction, Fig. 3. From the calculated phonon transmission probabilities I determine (adapting Ref. 14) the single-Si/Ge interface and thermal-barrier conductances

$$\sigma_{K,\text{TSB},\text{TDB}} = \sum_m \int \frac{d^2q}{(2\pi)^2} \times \left[\int_{\omega_{\min}}^{\omega_{\max}} \frac{d\omega}{2\pi} \hbar \omega T_{K,\text{TSB},\text{TDB}}(\omega; \alpha_q) \left(\frac{dN}{d\Theta} \right) \right]_m \quad (3)$$

by summing up the contributions at different modes $m = \xi_p, \xi_{x,y}$ and in-plane momenta q . In the result (3) ω_{\min} and ω_{\max} represent a shorthand for the corresponding frequency-integration limits $\omega_{\text{Si},\min}(\alpha_q)$ and $\omega_{\text{Si}(\text{Ge}),\max}(\alpha_q)$. I stress that the condition (2) must be absolutely satisfied to obtain a transport contribution to the interface conductance σ_K and effectively satisfied for the TSB and TDB conductances $\sigma_{\text{TSB},\text{TDB}}$ (however, all TSB and TDB-transport contributions are retained in the calculations reported here).

The top panel of Fig. 3 illustrates the general validity of the “classical” thermal-conductance approximation, Eq. (1), and documents the additional temperature variation produced by the low-energy Fabry-Perot resonances. The panel shows that the thermal-barrier conductance σ_{TSB} (solid curve) at all temperatures is comparable to and generally smaller than the individual Si/Ge-interface conductance σ_K (dotted curve).

The insert panel compares the corresponding phonon transmission probability $T_{\text{TSB}}(\omega)$ (calculated for Si/3Ge/Si at $q=0$) and the single-Si/Ge-interface transmission (dotted curve). The insert motivates the estimate (1) by emphasizing that (a) the thermal single-barrier transport is effectively restricted to incoming Si modes that satisfy the condition (2) (exactly as was found for the TDB transport, Fig. 2) and (b) the single-interface transmission (dotted curve) approximates the *average* thermal-barrier transmission

$$\langle T_{\text{TSB}}(\omega) \rangle \sim \langle T_K(\omega) \rangle \approx T_{\text{Si/Ge}}^0 \equiv \frac{4Z_{\text{Si}}Z_{\text{Ge}}}{(Z_{\text{Si}} + Z_{\text{Ge}})^2}, \quad (4)$$

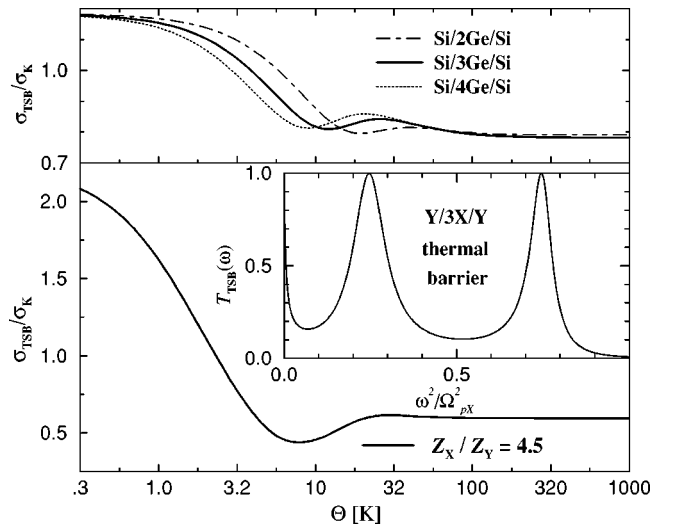


FIG. 4. Robustness (top panel) and enhancement (bottom panel) of the resonant-thermal-transport effects. The figure reports calculations of the thermal conductance ratio $\sigma_{\text{TSB}}/\sigma_K$ for both a set of Si/Ge/Si systems with different numbers of layers in the Ge barrier, and a fictitious X/3-Y-monolayer/X TSB structure with the significantly larger acoustic-impedance ratio $Z_X/Z_Y \approx 4.5$.¹⁸ The top panel documents that the predicted TSB resonant-thermal-transport effect is robust as the set of different barrier thicknesses produce qualitatively identical oscillations in the temperature variation of the TSB thermal-conductance ratio. The insert and bottom panels show that increasing the ratio of acoustic impedances causes much stronger Fabry-Perot resonances in the TSB transmission and an amplification of the thermal-conductance oscillations with temperature.

specified by the differences in acoustic impedances, $Z_{\text{Ge}}/Z_{\text{Si}} \approx 1.5$:¹⁵ $T_{\text{Si/Ge}}^0 \approx 0.95$. The observations (a) and (b) complete the argument (proof) for the “classical” thermal-conductance estimate (1).

The bottom panel of Fig. 3 documents that the phonon Fabry-Perot resonances refine the classical estimate (1) in producing resonant-thermal-transport effects. These arise at higher temperatures and in a more general and technologically relevant group of structures than the previously investigated case of dielectric quantum wires, Ref. 12. Specifically, the bottom panel of Fig. 3 details quantum oscillations in the temperature variations for both $\sigma_{\text{TSB}}/\sigma_{\text{K}}$ (solid curve) and $\sigma_{\text{TDB}}/\sigma_{\text{K}}$ (dashed curve). In both structures the thermal-conductance oscillations enhance as $T \rightarrow 0$ where the $T_{\text{TSB}}(\omega)$ and $T_{\text{TDB}}(\omega)$ variation increases in relative importance.

Finally, Fig. 4 emphasizes that the resonant-thermal-transport effects are robust against variations in the barrier thickness and enhance with an increasing ratio of the acoustic impedances of the TSB and TDB heterostructures. The figure reports calculations of the thermal-conductance variation both for a set of Si/Ge/Si systems and in a fictitious TSB

structure¹⁸ $X/3Y/X$, where $Z_X/Z_Y \approx 4.5$. The latter change produces a barrier transmission (insert panel) where the Fabry-Perot resonances cause a much more dramatic deviation from the average transmission approximated by the long-wavelength single-interface estimate (4), $\langle T_{\text{K}}(\omega) \rangle \sim 0.6$.

In summary, I have investigated the phonon transport perpendicular to the interfaces of (silicon/triple-germanium-layer/silicon) TSB and corresponding TDB structures. I document a strong suppression of the finite-temperature heterostructure thermal conductances σ_{TSB} and σ_{TDB} which approximately are limited by the conductance σ_{K} of an individual Si/Ge interface. In addition, I predict quantum oscillations in the thermal-conductance ratios $\sigma_{\text{TSB}}/\sigma_{\text{K}}$ and $\sigma_{\text{TDB}}/\sigma_{\text{K}}$ which arise from phonon Fabry-Perot resonances trapped in the central barrier or double-barrier region, respectively.

Discussions with G. D. Mahan are gratefully acknowledged. This work was supported by the Swedish Foundation for Strategic Research (SSF) through ATOMICS.

-
- ¹D.G. Cahill, W.K. Ford, K.E. Goodson, G.D. Mahan, A. Majumdar, H.J. Maris, R. Merlin, and S.R. Phillpot, *J. Appl. Phys.* **93**, 793 (2003).
- ²L.D. Hicks and M.S. Dresselhaus, *Phys. Rev. B* **47**, 12 727 (1993); G.D. Mahan and H.B. Lyon, Jr., *J. Appl. Phys.* **76**, 1899 (1994); J.O. Sofo and G.D. Mahan, *Appl. Phys. Lett.* **65**, 2690 (1994); D.A. Broido and T.L. Reinecke, *Phys. Rev. B* **51**, 13 797 (1995).
- ³G.D. Mahan and L.M. Woods, *Phys. Rev. Lett.* **80**, 4016 (1998).
- ⁴T. Yao, *Appl. Phys. Lett.* **51**, 1798 (1987).
- ⁵X.Y. Yu, G. Chen, A. Verma, and J.S. Smith, *Appl. Phys. Lett.* **67**, 3554 (1995).
- ⁶P. Hyldgaard and G.D. Mahan, in *Thermal Conductivity* (Technomic Publishing Company, Lancaster, Pennsylvania, 1996), Vol. 23, pp. 172–182.
- ⁷G. Chen, *J. Heat Transfer* **119**, 220 (1997).
- ⁸G. Chen, C.L. Tien, X. Wu, and J.S. Smith, *J. Heat Transfer* **116**, 325 (1994); W.S. Capinski and H.J. Maris, *Physica B* **219/220**, 699 (1996).
- ⁹S.M. Lee, D.G. Cahill, and R. Venkatasubramanian, *Appl. Phys. Lett.* **70**, 2957 (1997).
- ¹⁰S.Y. Ren and J.D. Dow, *Phys. Rev. B* **25**, 3750 (1982); A. Balan-
din and K.L. Wang, *ibid.* **58**, 1544 (1998).
- ¹¹P. Hyldgaard and G.D. Mahan, *Phys. Rev. B* **56**, 10 754 (1997).
- ¹²L.G.C. Rego and G. Kirczenow, *Phys. Rev. Lett.* **81**, 232 (1998); K. Schwab, E.A. Henriksen, J.M. Worlock, and M.L. Roukes, *Nature (London)* **404**, 974 (2000).
- ¹³Phonon Fabry-Perot resonances arise from partial reflection at the interfaces in the barrier structures. The corresponding photon concept is discussed, for example, in M. Young, *Optics and Lasers* (Springer-Verlag, Berlin, 1992), p. 136.
- ¹⁴S. Pettersson and G.D. Mahan, *Phys. Rev. B* **42**, 7386 (1990); R.J. Stoner and H.J. Maris, *ibid.* **48**, 16 373 (1993).
- ¹⁵V. Narayanamurti *et al.*, *Phys. Rev. Lett.* **43**, 2012 (1979); S. Mizuno and S.I. Tamura, *Phys. Rev. B* **45**, 734 (1992).
- ¹⁶I fit the values of $F_{p,t;\text{Si}}$ and $F_{p,t;\text{Ge}}$ to match the (long-wavelength) [100] sound velocities of the Si and Ge longitudinal and transverse modes as described in Ref. 11.
- ¹⁷P. Hyldgaard, *Mater. Sci. Eng., C* **23**, 243 (2003); *Low Temp. Phys.* **27**, 585 (2001); V. Narayanamurti, *Science* **213**, 717 (1981).
- ¹⁸The impedance ratio $Z_X/Z_Y \approx 4.5$ is very large but would characterize the phonon transport in a hypothetical Mg/triple-Hf-monolayer/Mg structure.